Identification of a Recognizable Progressive Skeletal Dysplasia Caused by *RSPRY1* Mutations

Maha Faden,[1,12] Fatema AlZahrani,[2,12] Roberto Mendoza-Londono,[3,4,12] Lucie Dupuis,[3,4] Taila Hartley,[5] Peter Kannu,[3,4] Julian A. Raiman,[3] Andrew Howard,[4,6] Wen Qin,[5] Martine Tetreault,[7,8] Joan Qiongchao Xi,[9] Imadeddin Al-Thamer,[10] Care4Rare Canada Consortium, Richard L. Maas,[9] Kym Boycott,[5] and Fowzan S. Alkuraya[2,11,*]

Skeletal dysplasias are highly variable Mendelian phenotypes. Molecular diagnosis of skeletal dysplasias is complicated by their extreme clinical and genetic heterogeneity. We describe a clinically recognizable autosomal-recessive disorder in four affected siblings from a consanguineous Saudi family, comprising progressive spondyloepimetaphyseal dysplasia, short stature, facial dysmorphism, short fourth metatarsals, and intellectual disability. Combined autozygome/exome analysis identified a homozygous frameshift mutation in *RSPRY1* with resulting nonsense-mediated decay. Using a gene-centric "matchmaking" system, we were able to identify a Peruvian simplex case subject whose phenotype is strikingly similar to the original Saudi family and whose exome sequencing had revealed a likely pathogenic homozygous missense variant in the same gene. *RSPRY1* encodes a hypothetical RING and SPRY domain-containing protein of unknown physiological function. However, we detect strong RSPRY1 protein localization in murine embryonic osteoblasts and periosteal cells during primary endochondral ossification, consistent with a role in bone development. This study highlights the role of gene-centric matchmaking tools to establish causal links to genes, especially for rare or previously undescribed clinical entities.

Skeletal dysplasias are a relatively common group of disorders involving the skeletal system with an estimated birth prevalence of 3 per 10,000.[1] The resulting physical and radiographic phenotype is highly variable and ranges from embryonic lethality to very mild phenotypes that might not come to medical attention. Major efforts to compartmentalize these disorders into clinically and radiologically recognizable entities to facilitate the study of their pathogenesis and natural history have led to the Nosology and Classification of Genetic Skeletal Disorders, which currently include 456 distinct disease headings.[2]

The extreme phenotypic heterogeneity of skeletal dysplasias pose a practical challenge in arriving at the correct diagnosis, which until recently was a pre-requisite for the establishment of the underlying genetic cause. Recently, genomic tools have proven very effective in uncovering causal mutations even in cases where no specific clinical diagnosis could be established, thereby ushering in the era of "genotype first" approach.[3,4] This approach has proven extremely valuable in such heterogeneous disorders as neurogenetic diseases.[5,6] Recently, we have shown in a large study that previously established OMIM genes account for fewer than 50% of skeletal dysplasia cases, which suggests that many more novel disease-gene links have yet to be established.[7] In this study, we describe a distinct and clinically recognizable skeletal dysplasia and show that this condition is probably caused by biallelic mutations in *RSPRY1* through a combination of exome sequencing, autozygome analysis, and gene-centric matchmaking.

The index individual (family 1_IV:3) is a 13-year-old Saudi girl who presented with short stature and progressive inability to walk. Her Bedouin family lives a nomadic life in the desert and had largely avoided contact with the medical system. She was a product of full-term NSVD after an uneventful pregnancy. She has history of delayed motor milestones, walking at 5 years of age but now wheelchair bound after she progressively lost the ability to walk. Her cognitive development was significantly delayed but she never had a formal IQ assessment. She can follow simple commands and her expressive language is severely limited. The family history is significant for first-degree consanguinity between the healthy parents and the presence of three similarly affected siblings who had not been brought to medical attention (Figure 1). Physical examination revealed poor weight gain (18 kg, −4.2 SD), severe short stature (100 cm, −8.2 SD), microcephaly (48 cm, −4.4 SD) with flattened occiput, and facial dysmorphism (hypertelorism, epicanthal folds, mild ptosis, strabismus, malar hypoplasia, short nose, depressed nasal bridge, full lips, small low-set ears, and short neck). Musculoskeletal examination was remarkable for short hands, malformed feet (rocker

[1]Department of Pediatrics, King Saud Medical Complex, Riyadh 11196, Saudi Arabia; [2]Department of Genetics, King Faisal and Research Center, Riyadh 11211, Saudi Arabia; [3]Division of Clinical and Metabolic Genetics, Department of Pediatrics, The Hospital for Sick Children and University of Toronto, Toronto, ON M5G 1X8, Canada; [4]The Bone Health Centre, The Hospital for Sick Children and University of Toronto, Toronto, ON M5G 1X8, Canada; [5]Children's Hospital of Eastern Ontario Research Institute, University of Ottawa, Ottawa, ON K1H 8L1, Canada; [6]Division of Orthopedic Surgery, The Hospital for Sick Children and University of Toronto, Toronto, ON M5G 1X8, Canada; [7]Department of Human Genetics, McGill University, Montreal, QC H3A 0G4, Canada; [8]McGill University and Genome Quebec Innovation Center, Montreal, QC H3A 0G4, Canada; [9]Division of Genetics, Department of Medicine, Brigham and Women's Hospital and Harvard Medical School, Boston, MA 02115, USA; [10]Deparment of Radiology, King Saud Medical Complex, Riyadh 11196, Saudi Arabia; [11]Department of Anatomy and Cell Biology, College of Medicine, Alfaisal University, Riyadh 11533, Saudi Arabia
[12]These authors contributed equally to this work
*Correspondence: falkuraya@kfshrc.edu.sa
http://dx.doi.org/10.1016/j.ajhg.2015.08.007.

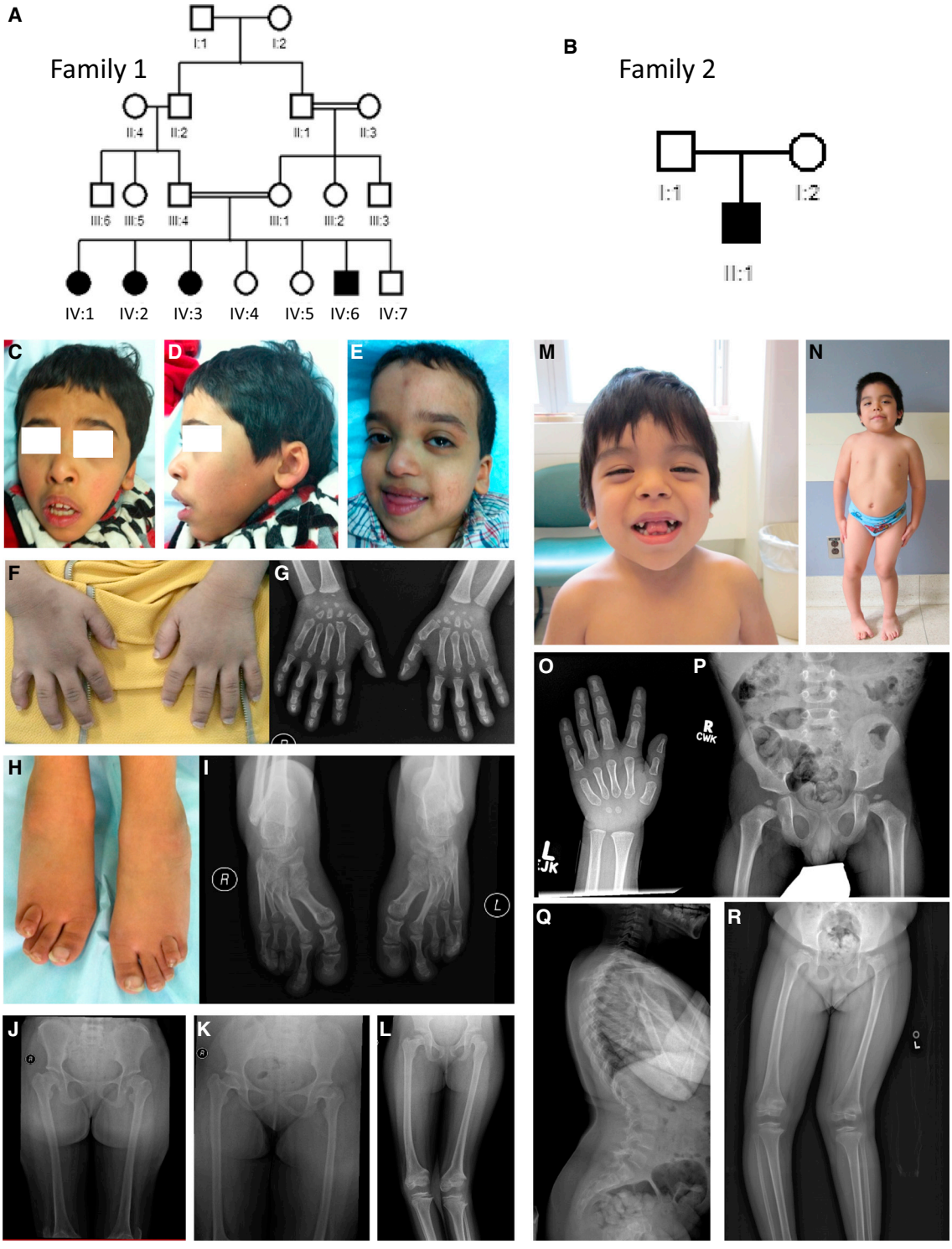

Figure 1. Identification of a Distinct Skeletal Dysplasia Syndrome
(A and B) Pedigrees of families 1 and 2.
(C and D) Facial images of family 1_IV:3 showing hypertolerism, epicanthal folds, partial ptosis, squint, malar hypoplasia, short nose, depressed nasal bridge, full lips, and short neck.
(E) Facial image of family 1_IV:6 showing frontal bossing, hypertolerism, partial ptosis but no squint, prominent cheeks with visible small vessels, short nose, mild depressed nasal bridge, full lips, low-set ears, and short neck.
(F) Hands of family 1_IV:3 are short and broad with short fingers and dysplastic nails.
(G) Hand radiographs of family 1_IV:6 showing small epiphysis of the both radius and ulna, mild irregularities of the metaphyses, and small-for-age carpal bones (micro carpal bones).
(H) Feet of family 1_IV:3 showing proximal insertion of the fourth toe that overlaps the third toe, lateral deviation of the big toe, dysplastic toenails, and partial syndactyly of the second and third toes.

(legend continued on next page)

Table 1. Summary of the Clinical and Radiographic Features of the Two Study Families

	Family 1				Family 2
	IV:1	IV:2	IV:3	IV:6	II:1
Gender	F	F	F	M	M
Age at assessment (years)	18	16	13	9.5	7.5
Short stature	+	+	+	+	+
ID	+	+	+	+	±
Delayed motor development	+	+	+	+	+
Delayed bone age	+	+	+	+	+
Microcephaly	+	+	+	+	+
Facial dysmorphism	+	+	+	+	+
Overriding toes	+	+	+	+	+
Scoliosis	+	+	+	+	+
Craniosynostosis	+	+	+	+	−
Small carpal bones	+	+	+	+	+
Platyspondyly	+	+	+	+	+
Coxa deformity	+	+	+	+	+
Genu deformity	+	+	+	+	+
Short femoral neck	+	+	+	+	+
Short fourth metatarsal	+	+	+	+	+
Cupped and frayed metaphysis	+	+	+	+	+

bottom heel with overriding toes), knocked knees, and mild scoliosis. There was generalized hypotonia with preserved deep tendon reflexes and reduced muscle power. Skeletal survey revealed generalized osteopenia, copper-beaten appearance of the skull with premature closure of sutures, short metacarpal bones, delayed bone age, platyspondyly, anterior wedging and posterior scalloping of the lower thoracic vertebras, and mild-moderate thoracolumber scoliosis. In addition, there was evidence of narrow pelvis, bilateral coxa vara, increased right acetabular angle, short and slender long bones, small epiphysis, cupping and fraying of the metaphyses of the tibia and fibula, slipped capital femoral epiphyses, short femoral neck, and mild distal femoral bowing. Subluxation of the left patella and a small non-ossified fibroma in the left femur were also noted. Importantly, the overriding toes were found to be secondary to marked shortening of the fourth metatarsal bilaterally. Parents subsequently brought the three reportedly affected siblings for medical evaluation and all had strikingly similar clinical and radiographic findings as summarized in Table 1 and Figure 1. Interestingly, the severity of the skeletal dysplasia appeared to correlate with the age e.g., the findings in the 18-year-old sister were more severe than those in the 9-year-old brother. We were able to perform a limited set of additional tests such as CT brain in the index individual, which revealed asymmetry of cerebral hemispheres, lateral ventricles, orbits, and skull, and there was evidence of premature closure of right coronal suture on 3D rendering of the CT skull. Ultrasound of abdomen and pelvis was normal as was cardiac echocardiogram and fundus examination.

The above findings suggested a highly distinct form of spondyloepimetaphyseal dysplasia (SEMD), most likely autosomal recessive in inheritance. Therefore, we recruited the family under an IRB-approved research protocol (KFSRHC RAC# 2080006), obtained written informed consent, and drew blood in EDTA and PAXGene tubes for DNA and RNA extraction, respectively. Autozygome analysis was performed as described before.[8,9] In brief, DNA from all family members was run on Axiom SNP Chip (Affymetrix) for genome-wide genotyping according to the manufacturer's protocol. The resulting genotyping files were interrogated for runs of homozygosity that are >1 Mb in size as surrogates of autozygosity using AutoSNPa.[10] Only two autozygous blocks were found to be exclusively shared by the affected members of the family. The first is chr16: 17,909,383–31,695,263 and the other is chr16: 52,478,215–58,313,806 (Figure 2). Both loci were further verified by linkage analysis performed with easyLINKAGE[11] (Figure 2). None of the 405 genes within these two intervals is known to cause a similar phenotype when mutated. Therefore, we proceeded with whole exome sequencing using DNA from the index individual. Exome capture was performed with TruSeq Exome Enrichment kit (Illumina) according to the manufacturer's protocol. Samples were prepared as an Illumina sequencing library, and in the second step, the sequencing libraries were enriched for the desired target with the Illumina Exome Enrichment protocol. The captured libraries were sequenced with Illumina HiSeq 2000 Sequencer. The reads are mapped against the UCSC Genome Browser. The SNPs and indels were detected by SAMTOOLS. We considered only very rare (MAF < 0.001) coding/splicing homozygous variants within the two critical autozygous intervals (Figure 2). The only variant that fit this definition was a homozygous 1 bp duplication in *RSPRY1* that predicts

(I) Foot radiographs of family 1_IV:1 showing severely short third and fourth metacarpals.
(J–L) Radiographs of family 1_IV:1 (J), 2 (K), and 3 (L) showing a remarkably similar pattern of bilateral coxa vara and small flat femoral epiphysis (genu valgum deformity is easily seen in L).
(M and N) Clinical photographs of family 2_II:1 at 5 (M) and 7.5 (N) years showing facial dysmorphism in the form of epicanthal folds, hypertelorism, short nose, tented upper lip, and low-set ears, as well as short neck and marked genu deformity.
(O) Hand radiograph showing small carpal bones.
(P) Pelvis radiograph showing immature flat femoral epiphysis.
(Q) Spine radiograph showing exaggerated lordosis with platyspondylyl.
(R) Marked genu deformity of both knees.

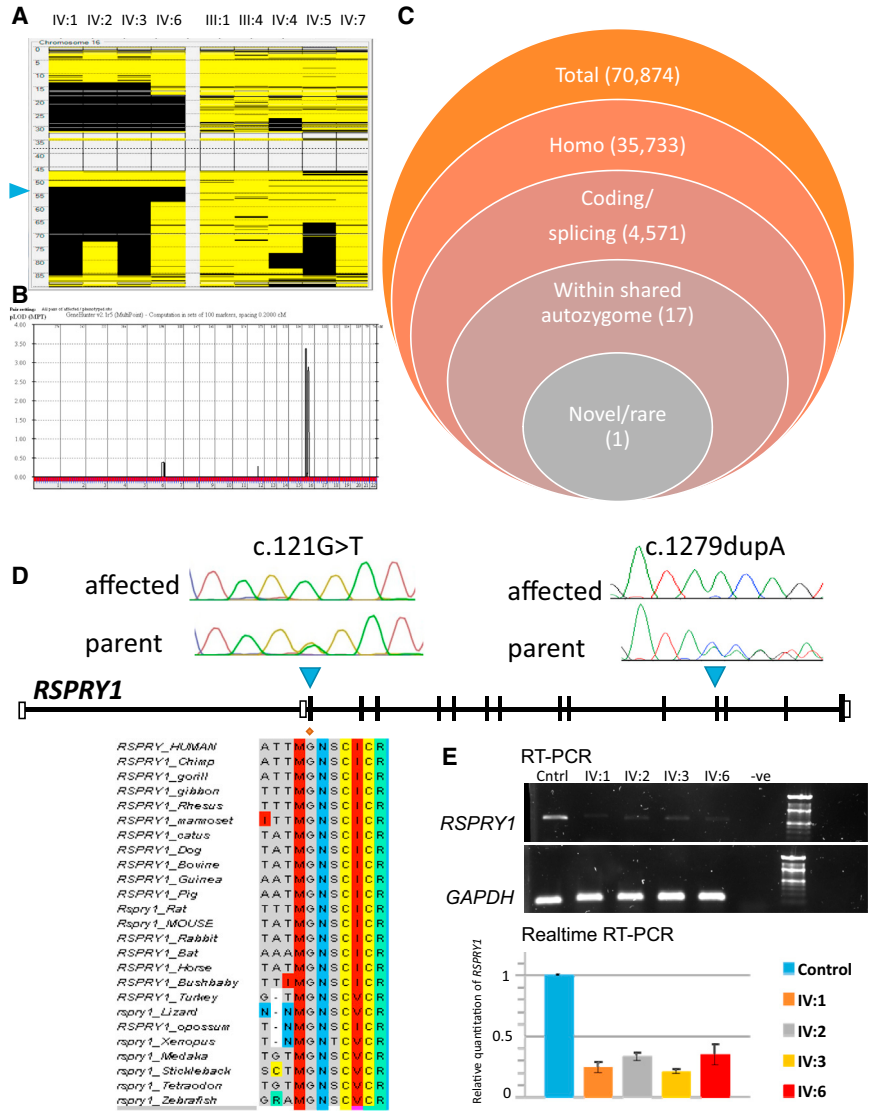

Figure 2. Identification of Mutations in *RSPRY1* in Families with a Distinct Skeletal Dysplasia Syndrome

(A) Output of AutoSNPa on family 1 showing the two critical autozygous intervals on chr16 that are exclusively shared by the affected members (*RSPRY1* locus indicated by blue triangle). Each column represents one sample (affected on the left and unaffected on the right) and each row represents the call of one SNP where black is homozygous and yellow is heterozygous.

(B) Genome-wide linkage analysis shows two adjacent peaks corresponding to the two ROHs shown in (A).

(C) Filtering strategy of the exomic variants generated on family 1_IV:1 showing a single surviving variant in *RSPRY1*.

(D) Cartoon of *RSPRY1* with the sequence chromatograms of the two mutations. The strong cross-species conservation of the mutated Gly41 residue in family 2 is also shown.

(E) Upper panel is the result of an RT-PCR experiment showing marked reduction of *RSPRY1* transcript as a result of NMD in the blood of affected members of family 1. Lower panel is the summary of two independent real-time RT-PCR experiments (each with technical triplicates) confirming the reduction of *RSPRY1* transcript in all affected members of family 1.

frameshift and premature truncation (GenBank: NM_133368.1; c.1279dupA [p.Thr427Asnfs*10]). Segregation of this variant with the disease was confirmed by Sanger sequencing in all family members. This variant is absent in 615 Saudi exomes, as well as the ExAC Consortium. Furthermore, RT-PCR revealed significant reduction (72% [46%–86%], $p < 0.0001$) of the *RSPRY1* transcript in blood of affected individuals compared to control subjects, most likely due to NMD (Figure 2).

As part of the collaboration between KFSHRC and Care4Rare Canada (both members of International Rare Disease Research Consortium [IRDiRC]), we had each established a matchmaking tool in which our respective databases could be screened for variants in likely disease-linked genes. The resulting matrix can then be queried whenever KFSHRC or Care4Rare Canada investigators identify a likely disease-causing variant in a gene not previously linked to disease. After failing to identify any match in KFSHRC matchmaking system, we queried the matchmaker at Care4Rare Canada and identified a single unsolved affected individual in whom exome sequencing had identified a homozygous deleterious-appearing variant in *RSPRY1*. Review of the clinical history, presentation, and radiological findings support the notion that these two affected individuals have similar phenotypes as detailed below.

The Care4Rare Canada index individual (family 2_II:1) was an 8-year-old male of Peruvian ancestry who presented to the genetics clinic for evaluation because of significant speech delay. He was the first and only pregnancy of a 36-year-old mother. This individual was delivered at 36 weeks gestation because of premature rupture of membranes. His birth weight was 2.85 kg. The parents deny known consanguinity but come from an isolated and small region in Peru and there is family history of a similar condition. Developmental delay was evidenced by his delayed walking until 23 months of age and inability to use a spoon and limited speech when he first presented at 3 years of age. He was formally assessed and diagnosed with autism spectrum disorder at 5 years of age. At 7.5 years of age, his expressive language was limited to 20 words that only people close to him recognize, but he was able to write his name.

When first examined at 3 years of age, his height was 91 cm (10^{th} centile), weight 14 kg (40^{th} centile), and head circumference 53.5 cm (+2.5 SD). His height showed

gradual deceleration with age; it was 91.5 cm at 4 years (−2.6 SD), 95.6 cm at 5 years (−2.8 SD), and 112.4 cm at 7.5 years (−4 SD). Throughout his follow-up visits, he had no corneal or lens clouding, no organomegaly, and normal male genitalia. Facial dysmorphic features included epicanthal folds, hypertelorism, short nose, tented upper lip, and low-set ears (Figure 1). Musculoskeletal examination revealed gradually increasing limited extension of the elbow, distal hyperextensibility, overriding toes, and short trunk with hyperlordosis. His skin was normal. At 8 years of age he developed significant valgus deformity of the left knee and varus deformity of the right knee necessitating surgical correction. The neurological examination revealed normal tone and power.

Skeletal survey at 3 years of age showed marked epiphyseal maturation defect. There was also some frontal bossing, steep floor of the cranial fossa, and mild cervical and thoracic platyspondyly. Skeletal survey at 5 years of age showed significant delay in epiphyseal maturation. The proximal ends of the metacarpals showed mild pointing of the proximal ends. In the pelvis there was flattened and irregular femoral heads with adequate coverage by the acetabulum. Mild scoliosis of the thoracolumbar spine was noted. Delayed epiphyseal maturation was also noted at 8 years of age along with flattening of femoral heads, thoracic platyspondyly, and short fourth metatarsals (Figure 2).

Urine was negative for glycosaminoglycans and oligosaccharides. Liver function tests, thyroid function tests, and basic blood biochemistry were consistently normal. Microarray analysis (aCGH) on an oligo array 44K platform was normal. Echocardiogram and abdominal ultrasound were normal. MRI of the brain at 5 years of age showed asymmetric prominent lateral ventricles with squaring off of the frontal horns and mild thinning of the anterior body of the corpus callosum. Light and electron microscopy of skin fibroblasts was normal.

Whole-exome sequencing was performed on genomic DNA after obtaining approval from the Institutional Review Board of the Hospital for Sick Children and informed consent from the family. DNA was captured with the SureSelect Human All Exon Kit v5 (Agilent Technologies) and sequenced on an Illumina HiSeq 2000 platform with paired-end 100 bp reads (McGill University and Genome Quebec Innovation Center). Read alignment to human genome hg19, variant calling, and annotation were done with a pipeline based on BWA (v.0.5.9), SAMtools (v.0.1.17), ANNOVAR, and custom annotation scripts as described previously.[12,13] Variants with possible protein altering effects (nonsense, frameshift, indel, splicing, and missense) with an allele frequency >1% in either the 1000 Genomes database or the NHLBI/NHGRI Exome Project (v.0.0.14, June 20, 2012), seen in >30 individuals in our exome database (more than 2,000 exomes), or that occurred as homozygotes in the ExAC database were excluded (Table S1). The final list of variants is listed in Table S2.

Based on the similarity in phenotype with the Saudi family, we were particularly interested in one rare homozygous missense variant (GenBank: NM_133368.1; c.121G>T [p.Gly41Cys]) in a conserved residue (GERP 5.22, Phast 658) in *RSPRY1* (Figure 2). This variant was not present in dbSNP, 1000 Genomes, the NHLBI/NHGRI Exome Project, or the ExAC database and was not previously seen in our in-house exome database. Moreover, the variant was predicted to be damaging by four different bioinformatics algorithms (SIFT [0.04], PolyPhen-2 [0.98], MutationTaster [0.99], and CADD [24.7]). Sanger sequencing confirmed that the variant was homozygous in the affected individual and that both parents were heterozygous.

As shown in Table 1, the affected individuals from both families have a strikingly similar clinical profile comprising overlapping facial dysmorphism, progressive SEMD, scoliosis, intellectual disability, brain asymmetry, and short fourth metatarsals. Craniosynostosis was observed in all four Saudi siblings but not in the Peruvian individual, so this might be another clinical feature of the disorder and its absence in the Peruvian individual might reflect the potentially milder effect of his missense mutation as compared to the null Saudi mutation. Nonetheless, there is sufficient clinical resemblance between the two families to conclude that they represent a single clinical entity, which we propose to be a distinct subtype of SEMD caused by loss of function of RSPRY1.

RSPRY1 is a protein with a RING and SPRY domains that is subjected to ubiquitination.[14–17] Although virtually nothing is known about the function of RSPRY1, we can make speculations based on other proteins known to contain the SPRY domain and might be relevant to the phenotype. For example, Sprouty1, 2, and 4 are all SPRY-containing proteins and inhibit FGF signaling. *Spry4* KO mice display dwarfism and abnormal digit development whereas *Spry2*/*Spry4* double KO mice have severe defects in craniofacial and limb development, probably mediated by enhanced FGF signaling.[18] Future work will clarify whether cells derived from individuals with *RSPRY1* mutations have enhanced FGF signaling, which might provide a mechanistic link to the associated phenotype.

To gain further evidence of causality for *RSPRY1* loss of function in the SEMD disorder observed in the Saudi and Canadian kindreds and insight into function, we examined the expression of *Rspry1* transcripts and the localization of the encoded protein by in situ hybridization, RT-PCR, and immunohistochemistry (IHC) in mid- to late-gestation mouse embryos and newborns. For IHC, we employed an affinity-purified rabbit polyclonal Novus antibody NBP1-92358, directed against residues 87–233 of full-length human RSPRY1, which contains only one amino acid difference from mouse in this region. The specificity of the RSPRY1 antibody via peroxidase or AP-coupled secondary antibody detection on paraffin and frozen sections was established by comparing *Rspry1* section in section in situ hybridization results by using a

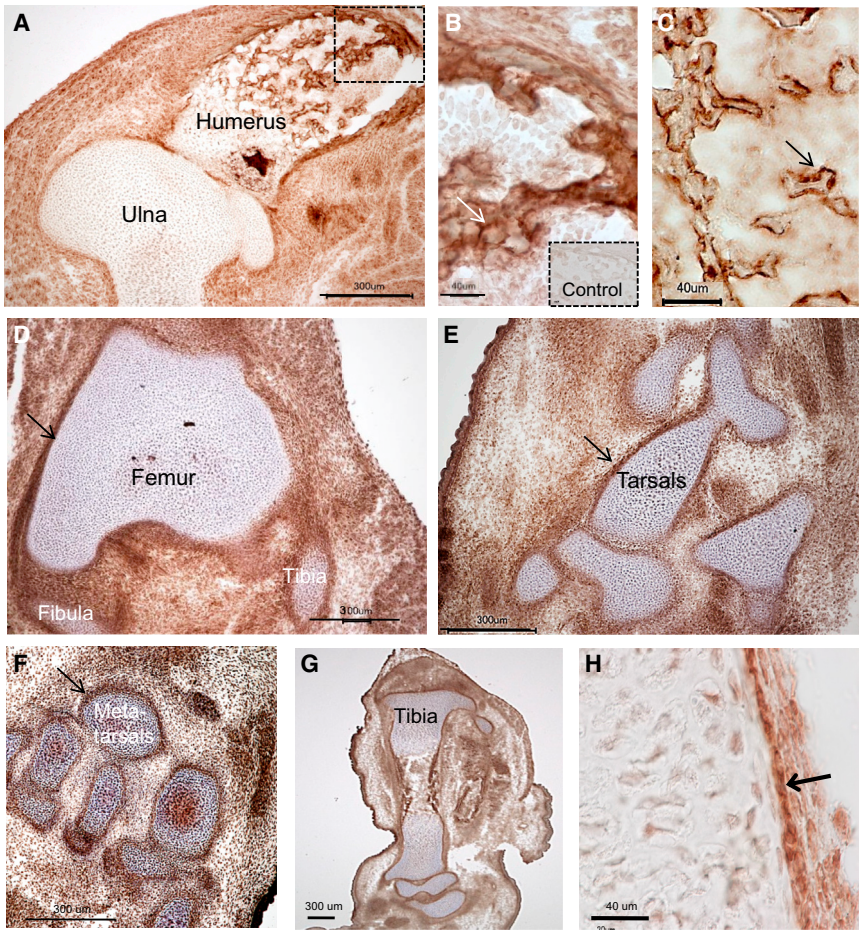

Figure 3. RSPRY1 Is Localized in Mouse Embryonic Bone and Surrounding Muscle Tissues during Primary Endochondral Ossification

(A–C) RSPRY1 protein localization in E18.5 mouse upper limb at the stylopod-zeugopod junction of the humerus and ulna (elbow). There is strong localization in the perichondrium and periosteum surrounding both bones and in presumptive osteoblasts and osteocytes (arrows) in developing cancellous bone in the humerus. Higher magnification shown in (B) (boxed region in A; with control staining of an IgG-treated section, inset) and (C), which represents a frozen section. Note the relative paucity of expression in hyaline cartilage in the ulna in (A) and strong expression in forelimb skeletal muscle surrounding both bones. Scale bars represent 300 μm in (A) and 40 μm in (B) and (C).

(D) RSPRY1 is strongly localized in distal femur perichondrial tissue at E18.5 (arrow). Note also staining in the fibromuscular connections to the fibula and tibia at the knee joint. Scale bar represents 300 μm.

(E and F) RSPRY1 localization in perichondrial tissues in tarsals (E) and metatarsals (F) (arrows) at E18.5, again coinciding with tissues affected in the described syndrome. Scale bars represent 300 μm.

(G and H) Tibial and tarsal localization of RSPRY1 at E18.5 in periosteum and perchondrium, the latter shown at higher magnification in (H). Note localization is stronger in a more internal perichondrial layer (arrow). Scale bars represent 200 μm in (G) and 40 μm in (H).

526 bp riboprobe to mouse *Rspry1* exon 15 3′ UTR with the IHC results in E12.5 mouse embryos.

Rspry1 transcripts and encoded protein were expressed in and localized to, respectively, intact mouse limb bud mesenchyme from as early as E12.5. At E18.5, coinciding with primary ossification in the mouse, RSPRY1 protein was abundantly detected in most developing endochondral bones and in skeletal muscles, as well as in developing heart, kidney, and brain (Figures 3A–3H and S1). In the E18.5 forelimb, RSPRY1 was detected in the humerus, ulna, radius, carpals, and metacarpals (Figures 3A–3C and S2). RSPRY1 was detected in similar fashion in the bones of the E18.5 hindlimb, including the femur, tibia, fibula, tarsals, and metatarsals (Figures 3D–3H). Strong localization was detected in both osteoblasts and osteocytes within these bones, with minimal localization in chondrocytes (Figures 3B and 3C). A second site of prominent RSPRY1 bone localization was in the perichondrium and periosteum, with the highest levels in the innermost, cellular layer (Figure 3H). In sum, the expression of *Rspry1* correlates strikingly with the skeletal defects observed in affected individuals and is also consistent with the presence of brain and craniofacial phenotypes, because expression was detected in embryonic and postnatal brain and in developing craniofacial tissues (Figure S1 and data not shown). Although the embryonic expression of *Rspry1* accounts for the presence of congenital skeletal dysplasia, further studies will be required to determine whether the progressive nature of the skeletal dysplasia in these families reflects a postnatal requirement for *Rspry1* osteogenic expression. In addition, the strong *Rspry1* expression in developing skeletal muscle raises the possibility that muscle defects might also contribute to the ambulatory defects in affected individuals.

Given the rate at which genes linked to Mendelian diseases have been identified since the introduction of genomic sequencing tools, it is inevitable that increasingly rare disorders will be the next frontier in gene discovery in the context of human diseases. For such rare disorders, especially novel ones, it is particularly challenging to achieve the gold standard of identifying more than one family with likely pathogenic mutations in the same gene and significant phenotype overlap to establish a causal disease-gene link. However, the increasing use of whole-exome and whole-genome sequencing in individuals with rare or novel phenotypes presents an opportunity for innovative matchmaking solutions. Some efforts have focused on phenotypic matchmaking via HPO terms;[19] however, the very well-established phenomenon of phenotypic variability in clinical genetics has the

potential to limit the usefulness of purely phenotype-driven tools. On the other hand, a gene-centric approach that allows matchmaking based on candidate genes can link the investigators who can then vet the phenotypic data in detail to make a conclusion regarding the degree of overlap. Indeed, the matching of the two families we present here is a good example of the power of the "genotype-first" matchmaking approach. Because the two groups of investigators (in Saudi Arabia and Canada) were linked through a matchmaking tool that took into account only the fact that we each had a candidate causal variant in *RSPRY1*, it was possible to conduct a thorough and joint analysis of the phenotype and conclude that it is very likely the same. A similar and large-scale approach based on genotype-driven matches is the web-based tool GeneMatcher, which links investigators with interest in the same gene.[20] Ideally, as we move forward, the development of more sophisticated matchmaking tools based on automated analysis of both phenotype and genotype will contribute significantly to the identification of the genes for these ultra-rare conditions. One such example of this type of approach is PhenomeCentral, and optimization and connection of these types of databases to each other will accelerate the pace of discovery.

In conclusion, we report a distinct subtype of SEMD characterized by severe short stature, facial dysmorphism, short fourth metatarsals, and intellectual disability with or without craniosynostosis. Our findings demonstrate that loss-of-function mutations in *RSPRY1* are the likely cause of this skeletal dysplasia, although the mechanism remains unclear. Our study highlights the usefulness of gene-centric matchmaking tools in accelerating the discovery of genes, especially for exceedingly rare or novel Mendelian disorders.

Supplemental Data

Supplemental Data include two figures and two tables and can be found with this article online at http://dx.doi.org/10.1016/j.ajhg.2015.08.007.

Acknowledgments

We thank the participating families for their enthusiastic participation. We thank the Genotyping and Sequencing Core Facilities at KFSHRC for technical help. This work was supported in part by King Salman Center for Disability Research grant (F.S.A.) and by a FaceBase Consortium grant from the National Institute of Dental and Craniofacial Research NIDCR U01DE024443 (F.S.A., R.L.M.). This disorder was selected for study by the Care4Rare Canada (Enhanced Care for Rare Genetic Diseases in Canada) Consortium Gene Discovery Steering Committee: Kym Boycott (lead; University of Ottawa), Alex MacKenzie (co-lead; University of Ottawa), Jacek Majewski (McGill University), Michael Brudno (University of Toronto), Dennis Bulman (University of Ottawa), and David Dyment (University of Ottawa). The study was funded, in part, by Genome Canada, the Canadian Institutes of Health Research, the Ontario Genomics Institute, Ontario Research Fund, Genome Quebec, Children's Hospital of Eastern Ontario Foundation, and the Hospital for Sick Children. The authors wish to acknowledge the contribution of the high throughput sequencing platform of the McGill University and Génome Québec Innovation Centre, Montréal, Canada and of Christopher Fay for assistance with the mouse expression studies. We also wish to thank Dr. Hichem Miaroui for helpful discussions pertaining to this manuscript.

Received: June 17, 2015
Accepted: August 10, 2015
Published: September 10, 2015

Web Resources

The URLs for data presented herein are as follows:

Burrows-Wheeler Aligner, http://bio-bwa.sourceforge.net/
CADD, http://cadd.gs.washington.edu/score
ExAC Browser, http://exac.broadinstitute.org/
IRDiRC, http://www.irdirc.org/
OMIM, http://www.omim.org/
PhenomeCentral, https://phenomecentral.org/
PolyPhen-2, http://genetics.bwh.harvard.edu/pph2/
SAMtools, http://samtools.sourceforge.net/
SIFT, http://sift.bii.a-star.edu.sg/
UCSC Genome Browser, http://genome.ucsc.edu

References

1. Stevenson, D.A., Carey, J.C., Byrne, J.L., Srisukhumbowornchai, S., and Feldkamp, M.L. (2012). Analysis of skeletal dysplasias in the Utah population. Am. J. Med. Genet. A. *158A*, 1046–1054.
2. Warman, M.L., Cormier-Daire, V., Hall, C., Krakow, D., Lachman, R., LeMerrer, M., Mortier, G., Mundlos, S., Nishimura, G., Rimoin, D.L., et al. (2011). Nosology and classification of genetic skeletal disorders: 2010 revision. Am. J. Med. Genet. A. *155A*, 943–968.
3. Lehner, B. (2013). Genotype to phenotype: lessons from model organisms for human genetics. Nat. Rev. Genet. *14*, 168–178.
4. Alkuraya, F.S. (2015). Natural human knockouts and the era of genotype to phenotype. Genome Med. *7*, 48.
5. Stessman, H.A., Bernier, R., and Eichler, E.E. (2014). A genotype-first approach to defining the subtypes of a complex disease. Cell *156*, 872–877.
6. Alazami, A.M., Patel, N., Shamseldin, H.E., Anazi, S., Al-Dosari, M.S., Alzahrani, F., Hijazi, H., Alshammari, M., Aldahmesh, M.A., Salih, M.A., et al. (2015). Accelerating novel candidate gene discovery in neurogenetic disorders via whole-exome sequencing of prescreened multiplex consanguineous families. Cell Rep. *10*, 148–161.
7. Alkuraya, F.; Saudi Mendeliome Group (2015). Comprehensive gene panels provide advantages over clinical exome sequencing for Mendelian diseases. Genome Biol. *16*, 134.
8. Alkuraya, F.S. (2010). Autozygome decoded. Genet. Med. *12*, 765–771.
9. Alkuraya, F.S. (2012). Discovery of rare homozygous mutations from studies of consanguineous pedigrees. Curr. Protoc. Hum. Genet. *Chapter 6*, 12.
10. Carr, I.M., Flintoff, K.J., Taylor, G.R., Markham, A.F., and Bonthron, D.T. (2006). Interactive visual analysis of SNP data for rapid autozygosity mapping in consanguineous families. Hum. Mutat. *27*, 1041–1046.

11. Lindner, T.H., and Hoffmann, K. (2005). easyLINKAGE: a PERL script for easy and automated two-/multi-point linkage analyses. Bioinformatics *21*, 405–407.
12. Fahiminiya, S., Majewski, J., Mort, J., Moffatt, P., Glorieux, F.H., and Rauch, F. (2013). Mutations in WNT1 are a cause of osteogenesis imperfecta. J. Med. Genet. *50*, 345–348.
13. McDonald-McGinn, D.M., Fahiminiya, S., Revil, T., Nowakowska, B.A., Suhl, J., Bailey, A., Mlynarski, E., Lynch, D.R., Yan, A.C., Bilaniuk, L.T., et al. (2013). Hemizygous mutations in SNAP29 unmask autosomal recessive conditions and contribute to atypical findings in patients with 22q11.2DS. J. Med. Genet. *50*, 80–90.
14. Povlsen, L.K., Beli, P., Wagner, S.A., Poulsen, S.L., Sylvestersen, K.B., Poulsen, J.W., Nielsen, M.L., Bekker-Jensen, S., Mailand, N., and Choudhary, C. (2012). Systems-wide analysis of ubiquitylation dynamics reveals a key role for PAF15 ubiquitylation in DNA-damage bypass. Nat. Cell Biol. *14*, 1089–1098.
15. Kim, W., Bennett, E.J., Huttlin, E.L., Guo, A., Li, J., Possemato, A., Sowa, M.E., Rad, R., Rush, J., Comb, M.J., et al. (2011). Systematic and quantitative assessment of the ubiquitin-modified proteome. Mol. Cell *44*, 325–340.
16. Wagner, S.A., Beli, P., Weinert, B.T., Nielsen, M.L., Cox, J., Mann, M., and Choudhary, C. (2011). A proteome-wide, quantitative survey of in vivo ubiquitylation sites reveals widespread regulatory roles. Mol. Cell. Proteomics *10*, 013284.
17. Danielsen, J.M., Sylvestersen, K.B., Bekker-Jensen, S., Szklarczyk, D., Poulsen, J.W., Horn, H., Jensen, L.J., Mailand, N., and Nielsen, M.L. (2011). Mass spectrometric analysis of lysine ubiquitylation reveals promiscuity at site level. Mol. Cell. Proteomics *10*, 003590.
18. Taniguchi, K., Ayada, T., Ichiyama, K., Kohno, R., Yonemitsu, Y., Minami, Y., Kikuchi, A., Maehara, Y., and Yoshimura, A. (2007). Sprouty2 and Sprouty4 are essential for embryonic morphogenesis and regulation of FGF signaling. Biochem. Biophys. Res. Commun. *352*, 896–902.
19. Gottlieb, M.M., Arenillas, D.J., Maithripala, S., Maurer, Z.D., Tarailo Graovac, M., Armstrong, L., Patel, M., van Karnebeek, C., and Wasserman, W.W. (2015). GeneYenta: a phenotype-based rare disease case matching tool based on online dating algorithms for the acceleration of exome interpretation. Hum. Mutat. *36*, 432–438.
20. Sobreira, N., Schiettecatte, F., Boehm, C., Valle, D., and Hamosh, A. (2015). New tools for Mendelian disease gene identification: PhenoDB variant analysis module; and GeneMatcher, a web-based tool for linking investigators with an interest in the same gene. Hum. Mutat. *36*, 425–431.